Andreev reflection and Aharonov–Bohm oscillations through a parallel-coupled double quantum dot with spin-flip scattering

2008 J. Phys.: Condens. Matter 20 465202

(http://iopscience.iop.org/0953-8984/20/46/465202)

IOP PUBLISHING JOURNAL OF PHYSICS: CONDENSED MATTER

J. Phys.: Condens. Matter **20** (2008) 465202 (6pp) doi:10.1088/0953-8984/20/46/465202

Andreev reflection and Aharonov–Bohm oscillations through a parallel-coupled double quantum dot with spin-flip scattering

Jin-Liang Li and Yu-Xian Li

College of Physics, Hebei Normal University, Shijiazhuang 050016, People's Republic of China
and
Hebei Advanced Film Laboratory, Shijiazhuang 050016, People's Republic of China

Received 18 July 2008, in final form 23 September 2008
Published 21 October 2008
Online at stacks.iop.org/JPhysCM/20/465202

Abstract

Using nonequilibrium Green's function techniques, we investigate Andreev reflection and Aharonov–Bohm oscillations through a parallel-coupled double quantum dot connected with a ferromagnetic lead and a superconductor lead. The possibility of controlling Andreev reflection and Aharonov–Bohm oscillations of the system is explored by tuning the interdot coupling, the gate voltage, the magnetic flux, and the intradot spin-flip scattering. When the spin-flip scattering increases, Fano resonant peaks resulting from the asymmetrical levels of the two quantum dots begin to split, and Aharonov–Bohm oscillations are suppressed. Due to the interdot coupling, one strongly and one weakly coupled state of the system can be formed. The magnetic flux can exchange the function of the two states, which leads to a swap effect.

(Some figures in this article are in colour only in the electronic version)

1. Introduction

Recent advances in nanotechnology have attracted much attention to the quantum coherence phenomena of resonant tunneling through quantum dot (QD) systems. To probe the coherence of an electron through a QD, interference experiments on the Aharonov–Bohm (AB) effect [1] in an AB interference with one QD in one of its arms have been done [2]. At the same time, the Kondo correlations [3–6] and the Fano effect [7, 8] have been addressed too. More recently, an AB interferometer containing two quantum dots has been realized [9–14], such as normal metal/double quantum dot/normal metal (N/DQD/N) [15], superconductor/double quantum dot/superconductor (S/DQD/S) [16], and so on. When the DQD system changes from the series to the symmetrical parallel configuration, the conductance is composed of Breit–Wigner and Fano line shapes at the bonding and antibonding energies, respectively, with their line broadenings controlled by the asymmetry of the configuration.

On the other hand, the mesoscopic hybrid structures of ferromagnet (F) and superconductor (S) [17–20] have some particular characters. Due to the appearance of the superconducting energy gap Δ, so-called Andreev reflection (AR) [21, 22] occurs. In the AR process, an electron incident with momentum k and spin σ picks up another electron with momentum $-k$ and spin $-\sigma$ to form a Cooper pair. It enters the S region and leaves an Andreev reflected hole in the F side. Currently, many research activities are being focused on the hybrid structures of F and S. The AR through the structure of F/DQ/S has been investigated by Cao *et al* [18]. Competition between the intradot spin-flip scattering and the tunneling coupling to the leads dominates the resonant behaviors of the Andreev reflection conductance. The spin-flip process can provide a bottleneck for the energy relaxation in the QD, i.e. for transitions between the excited and ground states [23]. A weak spin-flip scattering leads to a single-peak resonance. However, with increasing spin-flip scattering strength, the Andreev reflection conductance will develop into a double-peak resonance, indicating a novel structure in the conductance tunneling spectrum.

The DQD system is one of the promising candidates for a quantum bit in quantum computation by controlling the QD

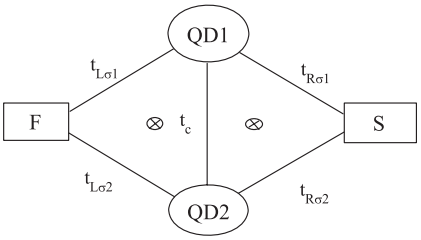

Figure 1. The model of a parallel-coupled double quantum dot system connected with an F lead and S lead.

levels [24]. When a parallel-coupled DQD connects to an F and an S lead, this system threaded by a magnetic flux is regarded as an AB interferometer; the transport properties, such as the Andreev conductance and the AB oscillations, can be controlled by the magnetic flux and the spin-flip scattering. Motivated by this, in this work, we calculate the spin-dependent AR through a parallel-coupled DQD system using nonequilibrium Green's function (NGF) techniques [25–28]. This parallel-coupled DQD structure is shown in figure 1. It is found that the AR conductance depends not only on the interdot coupling and the magnetic flux, but also on the spin-flip scattering. The interplay of the DQD and the F (S) lead provides new features in the electronic transport, which might throw some light on the potential of such structures as quantum devices.

The rest of this paper is organized as follows. In section 2, the model and the formulae for the DQD are introduced. Numerical results and discussions are shown in section 3. Section 4 consists of a brief conclusion.

2. Model and formulae

Consider a parallel-coupled double quantum dot system as shown in figure 1. The Hamiltonian of the system can be written as

$$H = H_{\rm F} + H_{\rm S} + H_{\rm DQD} + H_{\rm T}, \tag{1}$$

where $H_{\rm F}$ and $H_{\rm S}$ are the Hamiltonians for the F and the S leads.

$$H_{\rm F} = \sum_{k\sigma} (\varepsilon_{k\sigma} + \sigma \cdot h) a^{\dagger}_{k\sigma} a_{k\sigma}, \tag{2}$$

$$H_{\rm S} = \sum_{p\sigma} \varepsilon_{p\sigma} s^{\dagger}_{p\sigma} s_{p\sigma} + \sum_{p} (\Delta s^{\dagger}_{p\downarrow} s^{\dagger}_{-p\uparrow} + \Delta^{*} s_{p\uparrow} s_{-p\downarrow}). \tag{3}$$

Here, $a_{k\sigma}$ ($a^{\dagger}_{k\sigma}$) denotes the annihilation (creation) operator of the electron in the F lead with energy $\varepsilon_{k\sigma}$. An internal moment h is parallel to the F–QD interface. The BCS Hamiltonian is adopted for the S lead with Δ, which represents the S energy gap. $s_{p\sigma}$ ($s^{\dagger}_{p\sigma}$) denotes the annihilation (creation) operator of the electron in the S lead with energy $\varepsilon_{p\sigma}$. $H_{\rm DQD}$ models the parallel-coupled double quantum dot as

$$H_{\rm DQD} = \sum_{i\sigma} (\varepsilon_{i\sigma} - V_{{\rm g}i}) d^{\dagger}_{i\sigma} d_{i\sigma} + \sum_{\sigma} (t_{\rm c}\, {\rm e}^{{\rm i}\theta} d^{\dagger}_{1\sigma} d_{2\sigma} + {\rm hc}) + R \sum_{i} (d^{\dagger}_{i\uparrow} d_{i\downarrow} + {\rm hc}), \tag{4}$$

where $d_{i\sigma}$ ($d^{\dagger}_{i\sigma}$) denotes the annihilation (creation) operator of the electron with energy ε_i in the dot i ($i = 1, 2$), R is the spin-flip scattering strength, $t_{\rm c}$ denotes the interdot coupling strength, θ denotes a phase shift related to the flux difference between the left and the right subrings, and $V_{{\rm g}i}$ ($i = 1, 2$) represents the gate voltage, respectively. In this work, we ignore the intradot electron–electron Coulomb interaction and focus on the interdot coupling and the intradot spin-flip scattering. When the intradot Coulomb repulsion is considered, more peak structure develops in the conductance, with a characteristic Coulomb gap [29]. $H_{\rm T}$ represents the tunneling coupling between the DQD and leads

$$H_{\rm T} = \sum_{k,\sigma,i=1,2} (t_{k\sigma i} a^{\dagger}_{k\sigma i} d_{i\sigma} + {\rm hc}) + \sum_{p,\sigma,i=1,2} (t_{p\sigma i} s^{\dagger}_{p\sigma} d_{i\sigma} + {\rm hc}). \tag{5}$$

Here the tunneling matrix elements are set as $t_{k\sigma 1} = |t_{k\sigma 1}|\, {\rm e}^{{\rm i}\phi/4}$, $t_{k\sigma 2} = |t_{k\sigma 2}|\, {\rm e}^{-{\rm i}\phi/4}$, $t_{p\sigma 1} = |t_{p\sigma 1}|\, {\rm e}^{-{\rm i}\phi/4}$, and $t_{p\sigma 2} = |t_{p\sigma 2}|\, {\rm e}^{{\rm i}\phi/4}$. The phase shift due to the total magnetic flux threading into the AB ring is assumed to be $\phi = 2\pi(\phi_{\rm R} + \phi_{\rm L})/\phi_0$ with the flux quantum $\phi_0 = hc/e$, where $\phi_{\rm R/L}$ is the magnetic flux threading the right/left subring. The difference between the two parts of magnetic flux is $\theta = \pi(\phi_{\rm R} - \phi_{\rm L})/\phi_0$. If the ratio of the two magnetic fluxes is $n = \phi_{\rm R}/\phi_{\rm L}$, the phase associated with the two subrings of the mesoscopic ring can be expressed as $\phi_{\rm R} = \frac{n}{n+1}\phi$ and $\phi_{\rm L} = \frac{1}{n+1}\phi$. The difference between the two magnetic fluxes can be expressed as $\theta = \frac{n-1}{2(n+1)}\phi$. In the following calculation, we define the linewidth matrix as $\Gamma^{\alpha}_{ij} = \Sigma_k t_{\alpha i} t^{*}_{\alpha i} 2\pi\delta(\varepsilon - \varepsilon_{k\alpha})$; α represents L or R.

The electronic current passing through lead F is defined as

$$I_{\rm L} = e\left\langle \frac{{\rm d}N_{\rm L}}{{\rm d}t} \right\rangle = -\frac{e}{\hbar}\,{\rm Re} \sum_{k}^{i=1,3,5,7} T^{\dagger}_{k,ii} G^{<}_{k,ii}(t, t'), \tag{6}$$

with $N_{\rm L} = \Sigma_{k\sigma} a^{\dagger}_{k\sigma} a_{k\sigma}$. $G^{<}_{i\sigma,k\sigma}(t, t') = i\langle a^{\dagger}_{k\sigma}(t') d_{i\sigma}(t)\rangle$ is the lesser Green's function, which can be calculated with the retarded Green's function.

The Fourier transformed retarded Green's function of the system can be solved with Dyson's equation, $G^{\rm r} = G^{\rm r}_0 + G^{\rm r}_0 \Sigma^{\rm r} G^{\rm r}$, in which $G^{\rm r}_0$ is the free retarded Green's function for an isolated DQD and $\Sigma^{\rm r}$ is the self-energy matrix due to the tunneling coupling between the DQD and the leads. In the 8×8 generalized Nambu-spin space, the free Green's function $G^{\rm r}_0(\varepsilon)$ for the isolated DQD system is given by

$$G^{\rm r}_0(\varepsilon) = \begin{pmatrix} \varepsilon - \varepsilon_1 + \delta & 0 & R & 0 \\ 0 & \varepsilon + \varepsilon_1 + \delta & 0 & -R \\ R & 0 & \varepsilon - \varepsilon_1 + \delta & 0 \\ 0 & -R & 0 & \varepsilon + \varepsilon_1 + \delta \\ t_{\rm c}\, {\rm e}^{-{\rm i}\theta} & 0 & 0 & 0 \\ 0 & -t_{\rm c}\, {\rm e}^{{\rm i}\theta} & 0 & 0 \\ 0 & 0 & t_{\rm c}\, {\rm e}^{-{\rm i}\theta} & 0 \\ 0 & 0 & 0 & -t_{\rm c}\, {\rm e}^{{\rm i}\theta} \end{pmatrix}^{-1} \times \begin{pmatrix} t_{\rm c}\, {\rm e}^{{\rm i}\theta} & 0 & 0 & 0 \\ 0 & -t_{\rm c}\, {\rm e}^{-{\rm i}\theta} & 0 & 0 \\ 0 & 0 & t_{\rm c}\, {\rm e}^{{\rm i}\theta} & 0 \\ 0 & 0 & 0 & -t_{\rm c}\, {\rm e}^{-{\rm i}\theta} \\ \varepsilon - \varepsilon_2 + \delta & 0 & R & 0 \\ 0 & \varepsilon + \varepsilon_2 + \delta & 0 & -R \\ R & 0 & \varepsilon - \varepsilon_2 + \delta & 0 \\ 0 & -R & 0 & \varepsilon + \varepsilon_2 + \delta \end{pmatrix}^{-1}, \tag{7}$$

where $\delta = i0^{\dagger}$. $\Gamma_{\rm f}$ is the tunneling coupling matrix between the DQD and F lead and is written as follows:

$$\Gamma_{\rm f} = \begin{pmatrix} \Gamma_{1\uparrow} & 0 & 0 & 0 & \Gamma_{\uparrow}\,{\rm e}^{{\rm i}\phi/2} \\ 0 & \Gamma_{1\downarrow} & 0 & 0 & 0 \\ 0 & 0 & \Gamma_{1\downarrow} & 0 & 0 \\ 0 & 0 & 0 & \Gamma_{1\uparrow} & 0 \\ \Gamma_{\uparrow}\,{\rm e}^{-{\rm i}\phi/2} & 0 & 0 & 0 & \Gamma_{2\uparrow} \\ 0 & \Gamma_{\downarrow}\,{\rm e}^{{\rm i}\phi/2} & 0 & 0 & 0 \\ 0 & 0 & \Gamma_{\downarrow}\,{\rm e}^{-{\rm i}\phi/2} & 0 & 0 \\ 0 & 0 & 0 & \Gamma_{\uparrow}\,{\rm e}^{{\rm i}\phi/2} & 0 \end{pmatrix}$$

$$\begin{pmatrix} 0 & 0 & 0 \\ \Gamma_{\downarrow}\,{\rm e}^{-{\rm i}\phi/2} & 0 & 0 \\ 0 & \Gamma_{\downarrow}\,{\rm e}^{{\rm i}\phi/2} & 0 \\ 0 & 0 & \Gamma_{\uparrow}\,{\rm e}^{-{\rm i}\phi/2} \\ 0 & 0 & 0 \\ \Gamma_{2\downarrow} & 0 & 0 \\ 0 & \Gamma_{2\downarrow} & 0 \\ 0 & 0 & \Gamma_{2\uparrow} \end{pmatrix}. \quad (8)$$

Here, we set $\Gamma_{\uparrow} = \sqrt{\Gamma_{1\uparrow}\Gamma_{2\uparrow}}$ and $\Gamma_{\downarrow} = \sqrt{\Gamma_{1\downarrow}\Gamma_{2\downarrow}}$; $\Gamma_{i\sigma}$ ($i = 1, 2, \sigma = \uparrow, \downarrow$) is the linewidth function describing the coupling between the dot and the F lead. Under the wide-bandwidth approximation, the linewidth functions are independent of the energy. The self-energy from the tunneling coupling between the DQD and the F lead is $\Sigma_{\rm f}^{\rm r} = -(i/2)\Gamma_{\rm f}$.

It is useful to introduce the coupling matrix $\Gamma_{\rm s}$ between the DQD and the S lead

$$\Gamma_{\rm s} = \rho_{\rm s}^{\rm r}(w)\Gamma_{\rm s0} \times \begin{pmatrix} \Gamma_1^{\rm R} & -\Gamma_1\,{\rm e}^{-{\rm i}\phi/2} & 0 & 0 \\ -\Gamma_1\,{\rm e}^{{\rm i}\phi/2} & \Gamma_1^{\rm R} & 0 & 0 \\ 0 & 0 & \Gamma_1^{\rm R} & -\Gamma_1\,{\rm e}^{-{\rm i}\phi/2} \\ 0 & 0 & -\Gamma_1\,{\rm e}^{{\rm i}\phi/2} & \Gamma_1^{\rm R} \\ \Gamma^{\rm R}\,{\rm e}^{{\rm i}\phi/2} & -\Gamma^{\rm R}\frac{\Delta}{\varepsilon} & 0 & 0 \\ -\Gamma^{\rm R}\frac{\Delta}{\varepsilon} & \Gamma^{\rm R}\,{\rm e}^{-{\rm i}\phi/2} & 0 & 0 \\ 0 & 0 & \Gamma^{\rm R}\,{\rm e}^{{\rm i}\phi/2} & -\Gamma^{\rm R}\frac{\Delta}{\varepsilon} \\ 0 & 0 & -\Gamma^{\rm R}\frac{\Delta}{\varepsilon} & \Gamma^{\rm R}\,{\rm e}^{-{\rm i}\phi/2} \end{pmatrix}$$

$$\begin{pmatrix} \Gamma^{\rm R}\,{\rm e}^{-{\rm i}\phi/2} & -\Gamma^{\rm R}\frac{\Delta}{\varepsilon} & 0 & 0 \\ -\Gamma^{\rm R}\frac{\Delta}{\varepsilon} & \Gamma^{\rm R}\,{\rm e}^{{\rm i}\phi/2} & 0 & 0 \\ 0 & 0 & \Gamma^{\rm R}\,{\rm e}^{-{\rm i}\phi/2} & -\Gamma^{\rm R}\frac{\Delta}{\varepsilon} \\ 0 & 0 & -\Gamma^{\rm R}\frac{\Delta}{\varepsilon} & \Gamma^{\rm R}\,{\rm e}^{{\rm i}\phi/2} \\ \Gamma_2^{\rm R} & -\Gamma_2\,{\rm e}^{{\rm i}\phi/2} & 0 & 0 \\ -\Gamma_2\,{\rm e}^{-{\rm i}\phi/2} & \Gamma_2^{\rm R} & 0 & 0 \\ 0 & 0 & \Gamma_2^{\rm R} & -\Gamma_2\,{\rm e}^{{\rm i}\phi/2} \\ 0 & 0 & -\Gamma_2\,{\rm e}^{-{\rm i}\phi/2} & \Gamma_2^{\rm R} \end{pmatrix}. \quad (9)$$

Here $\Gamma_{\rm s0} = 2\pi\rho_{\rm s0}|T_{p\sigma}|^2$ is the tunneling coupling matrix between the DQD and the S lead; $\rho_{\rm s0}$ in $\Gamma_{\rm s0}$ is the density of states when the superconductor is in the normal state. $\Gamma_i^{\rm R}$ ($i = 1, 2$) is the linewidth function describing the coupling between the dot and the S lead. We set $\Gamma^{\rm R} = \sqrt{\Gamma_1^{\rm R}\Gamma_2^{\rm R}}$, $\Gamma_i = \Gamma_i^{\rm R}\frac{\Delta}{\varepsilon}$ ($i = 1, 2$). $\rho_{\rm s}^{\rm r}(w)$ is the modified dimensionless BCS density of states,

$$\rho_{\rm s}^{\rm r}(w) = \begin{cases} \dfrac{|w|}{\sqrt{w^2 - \Delta^2}} & |w| > \Delta, \\ \dfrac{w}{i\sqrt{\Delta^2 - w^2}} & |w| < \Delta. \end{cases} \quad (10)$$

The self-energy from the tunneling coupling between the DQD and the S lead, $\Sigma_{\rm s}^{\rm r} = -\frac{i}{2}\Gamma_{\rm s}$. By using the Dyson equation, the retarded Green function of the system is

$$G^{\rm r}(\varepsilon) = [G_0^{\rm r}(\varepsilon)^{-1} - \Sigma^{\rm r}(\varepsilon)]^{-1}, \quad (11)$$

where $\Sigma^{\rm r}(\varepsilon) = \Sigma_{\rm f}^{\rm r}(\varepsilon) + \Sigma_{\rm s}^{\rm r}(\varepsilon)$. Taking the Fourier transformation, the current formula becomes

$$J_{\rm L} = \frac{e}{h}\int {\rm d}w[f_{\rm l}(w - eV) - f_{\rm r}(w)] \sum_{i=1,3,5,7} [G^{\rm r}\Gamma_{\rm s}G^{\rm a}\Gamma_{\rm f}]_{ii} + \frac{e}{h}\int {\rm d}w[f_{\rm l}(w - eV) - f_{\rm r}(w + eV)] \times \sum_{i=1,3,5,7}^{j=2,4,6,8} [G^{\rm r}\Gamma_{\rm f}G^{\rm a}\Gamma_{\rm f}]_{ji}, \quad (12)$$

where $f_{\rm l}(w)$ and $f_{\rm r}(w)$ are the Fermi-distribution functions in the left and right leads, respectively. $G^{\rm a} = (G^{\rm r})^{\dagger}$ is the advanced Green's function. The first term of $J_{\rm L}$ is the normal tunneling current which is caused by the single quasiparticle or quasihole transport. The second term is the AR current. The normal linear conductance is zero at zero temperature, and the AR process contributes to the linear electronic transport of the system. The AR conductance can be calculated as

$$G_A = \frac{2e^2}{h}\sum_{i=1,3,5,7}^{j=2,4,6,8} G_{ij}^{\rm r}(\Gamma_{\rm f}G^{\rm a}\Gamma_{\rm f})_{ji}. \quad (13)$$

3. Results and discussion

In this work, we investigate the linear AR conductance at zero temperature for the F/DQD/S system, in which the Fermi energy of the two leads and the energy levels of the DQD are restricted in the range of the energy gap Δ of the S lead. The spin polarization in the F lead is defined as $p = (\Gamma_{\rm f\uparrow} - \Gamma_{\rm f\downarrow})/(\Gamma_{\rm f\uparrow} + \Gamma_{\rm f\downarrow})$, and the spin-averaged coupling strength is $\Gamma_{\rm f0} = (\Gamma_{\rm f\uparrow} + \Gamma_{\rm f\downarrow})/2$. The energy gap Δ of the S lead is taken as the energy unit and the spin polarization is chosen as $p = 0.3$.

First we discuss the interference effects in the transport with the symmetric DQD structure. Figure 2 shows the AR conductance versus Fermi energy with different spin-flip scattering strengths. In this case, we set $\varepsilon_1 = \varepsilon_2 = 0.1$, $\Gamma_{\rm f0} = \Gamma_{\rm s} = 0.1$, and $t_{\rm c} = 0.0$, respectively. The two quantum dots contribute to two separate channels, which allow the electrons to tunnel. When the spin-flip scattering is absent, i.e. $R = 0.0$, we can see from figure 2 that the AR conductance displays two Breit–Wigner resonances. With the spin-flip scattering R increasing, the two resonant peaks shift gradually towards the Fermi energy $\varepsilon = 0$. These unattached states are overlapped at $R = 0.1$, where the AR conductance displays one peak. Continue to increase R, and the single-peak conductance develops into a double-peak resonance again. Moreover, as the spin-flip scattering increases, the amplitudes of the two resonant peaks decrease and the distance between the two peaks becomes large. The intradot spin-flip scattering not only shifts the level position of the DQD, but also changes the spin-up and spin-down distribution of the density of states for the split levels. When $R > 0.15$ we can see from figure 2 that two new peaks appear beside the main resonances.

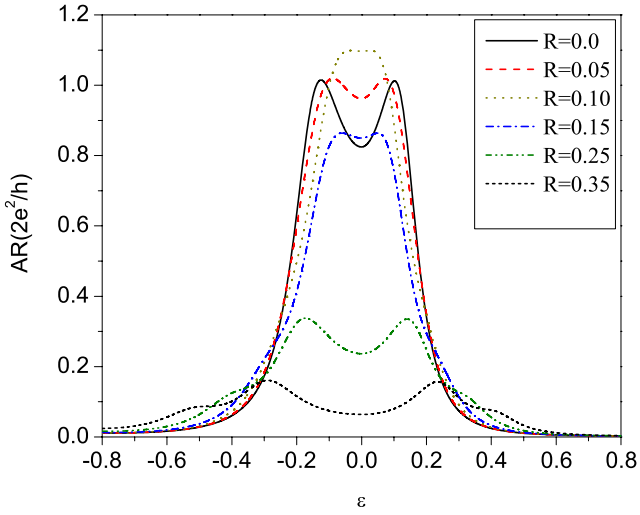

Figure 2. AR conductance as a function of the Fermi energy ε with different spin-flip scatterings R. $t_c = 0$, $\varepsilon_1 = \varepsilon_2 = 0.1$, and $\phi = \theta = 0$, respectively.

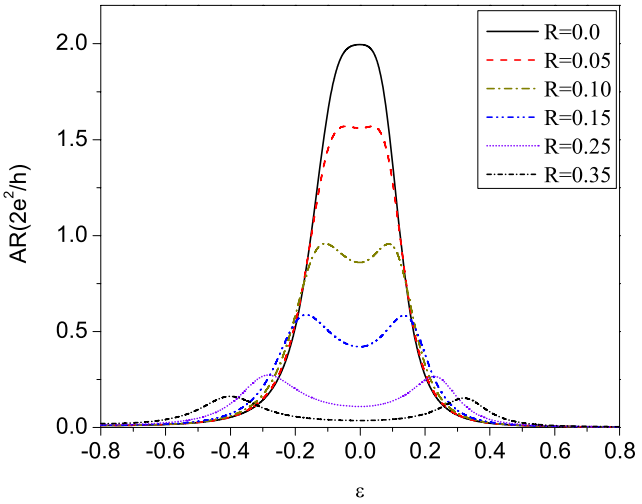

Figure 3. AR conductance as a function of the Fermi energy ε with different spin-flip scatterings R. $t_c = 0.1$; other parameters are as those in figure 2.

When the two QDs are coupled, the AR conductance with different values of spin-flip scattering is plotted in figure 3. The interdot coupling $t_c = 0.1$; the other parameters are the same as those in figure 2. The minority spin population near the Fermi energy determines the probability of the pairing. When $R = 0.0$, the electron resonant tunneling and the free spin-flip between the two dots lead to the minority spin population near the Fermi energy increasing; a perfect AR tunneling process occurs at $\varepsilon = 0$. If the spin-flip scattering is considered, it consumes more energy to make the electrons spin flip; the resonant tunneling and spin-flip of electrons are controlled between the two dots, then the peak of the AR conductance decreases gradually. When the spin-flip scattering strength varies from 0 to 0.05, the two split energies are overlapped effectively and the AR conductance behaves as a single-peak resonance. With R increasing, the two split energies are separated from each other, leaving an almost vanishing spin-dependent density of states at the Fermi energy, and as a result the conductance drops quickly to zero at $\varepsilon = 0$. At the same time, two resonance peaks occur in the AR conductance because of the resonant broadening of the two spin-coherent split levels $\varepsilon = \pm R$. The half width of the peak for each state broadens gradually.

When the interdot coupling is very strong, for example $t_c = 0.5$, the two coupled quantum dot levels are renormalized and are transformed into the bonding-like and antibonding-like states of an artificial molecule. In figure 4 we can find that interference effect is very clear. The intradot spin-flip scattering shifts the level position of the DQD $\varepsilon = \varepsilon \pm t_c$ to $\varepsilon = \varepsilon \pm t_c \pm R$, which results in four resonant peaks in the AR conductance. The original two resonant peaks shift towards the Fermi energy, and overlap effectively at $R = 0.45$. As a result, a single peak occurs in the AR conductance, with the maximum value $2e^2/h$ at $\varepsilon = 0$.

In order to show the effect of the interdot coupling on the quantum interference, we plot the AR conductance versus the interdot coupling t_c with different spin-flip scatterings; the

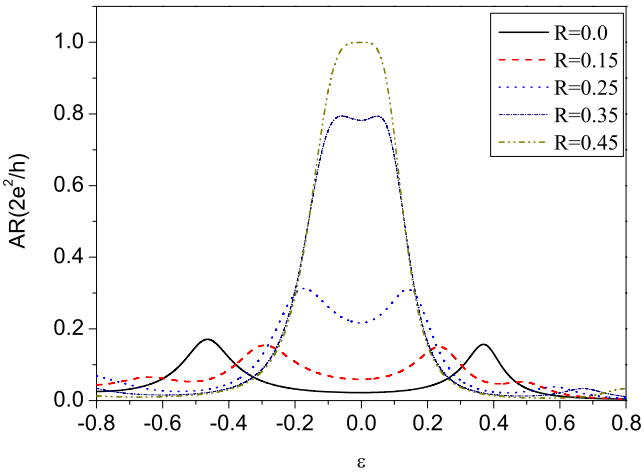

Figure 4. AR conductance as a function of the Fermi energy ε with different spin-flip scatterings R. $t_c = 0.5$; other parameters are as those in figure 2.

result is shown in figure 5. The AR conductance presents a resonant peak at $t_c = 0.1 + R$. When $R = 0$, a perfect AR tunneling process occurs at $t_c = 0.1$, which is the same as shown in figure 3. For a weak spin-flip scattering strength ($R < 0.09$), the AR conductance displays a single-peak resonance at $t_c = 0.1$ and its amplitude gradually decreases. It is worthwhile to notice that the spin-up and spin-down electrons are now coupled due to the combined effect of the interdot coupling and the intradot spin-flip scattering. We can see from the figure that two resonant states appear when the spin-flip scattering is about 0.09. With the spin-flip scattering increasing, the resonant tunneling needs a strong interdot coupling; the AR peaks shift to $t_c = 0.1 + R$.

It is interesting to show that when the quantum dots have different energy levels, for example $\varepsilon_1 = 0.1$, $\varepsilon_2 = -0.3$, with the interdot coupling $t_c = 0.5$, these two asymmetric quantum dot levels result in the Fano resonant peaks. Figure 6 shows that, without spin-flip scattering, i.e. $R = 0$, the

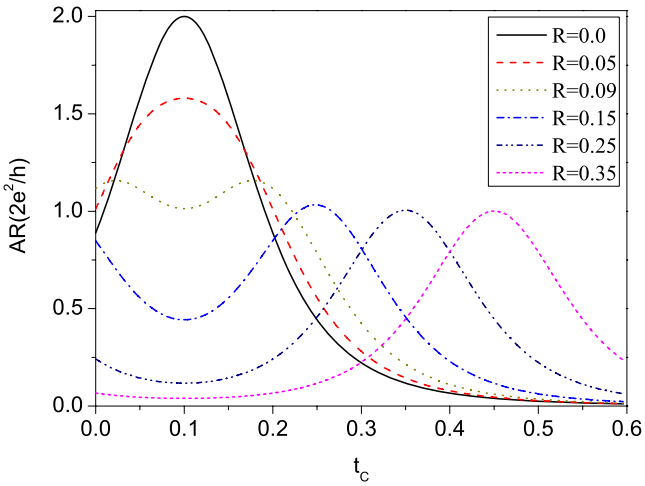

Figure 5. AR conductance as a function of the interdot coupling strength t_c, with different spin-flip scatterings R. $\varepsilon_1 = \varepsilon_2 = 0.1$, $\varepsilon = 0$, and $\phi = \theta = 0$.

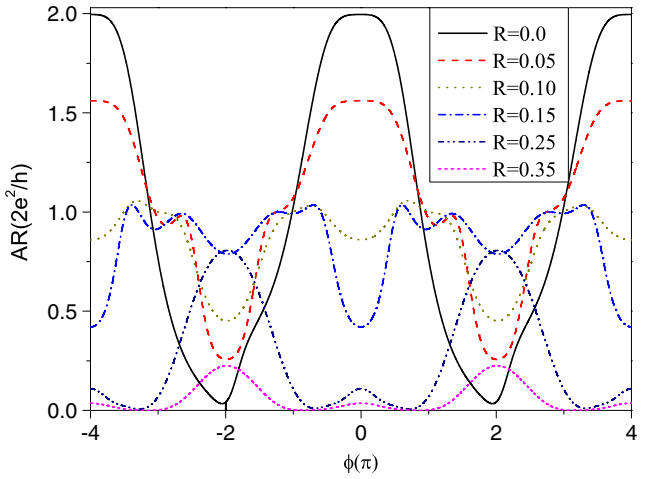

Figure 7. AR conductance as a function of the magnetic flux ϕ with different spin-flip scatterings R. $t_c = 0.1$, $\varepsilon_1 = 0.1$, $\varepsilon_2 = 0.1$, Fermi energy $\varepsilon = 0$, and $\theta = 0$, respectively.

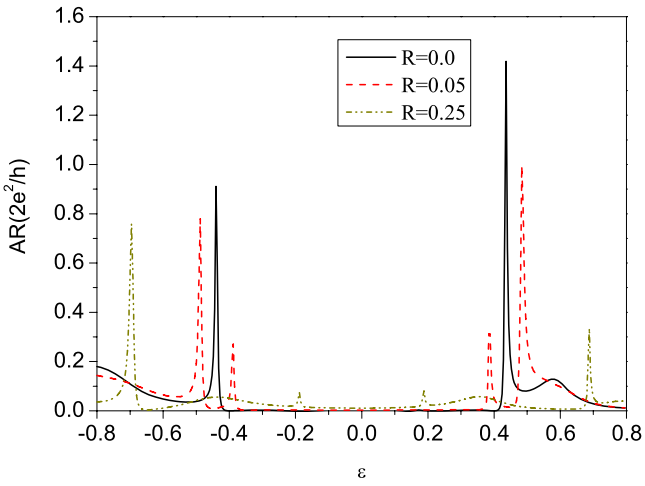

Figure 6. AR conductance as a function of the Fermi energy ε with different spin-flip scatterings R. $t_c = 0.5$, $\varepsilon_1 = 0.1$, $\varepsilon_2 = -0.3$, and $\phi = \theta = 0$, respectively.

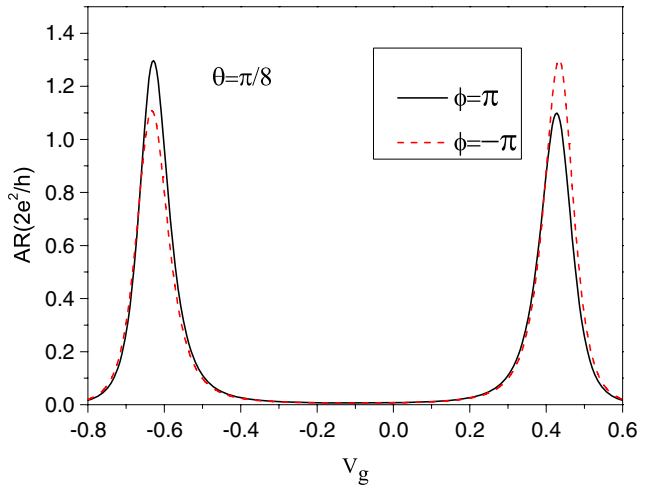

Figure 8. AR conductance as a function of gate voltage V_g. $t_c = 0.5$, $\varepsilon_1 = \varepsilon_2 = 0.1$, $\varepsilon = 0$, $R = 0$, $\theta = \pi/8$, respectively.

AR conductance indicates two Fano resonant peaks at $\varepsilon = \pm[\frac{\varepsilon_1+\varepsilon_2}{2} + t_c]$. Considering the spin-flip scattering, the two Fano peaks are split into four Fano resonances; the positions of the resonant states are about $\varepsilon = \pm[\frac{\varepsilon_1+\varepsilon_2}{2} + t_c \pm R]$; the Breit–Wigner resonance beside the Fano peak becomes weak. With the spin-flip scattering R increasing, the amplitudes of the Fano resonances decrease. However, if the spin-flip scattering is strong enough, for example $R = 0.25$, between the split Fano resonance we can find that another two Breit–Wigner resonances appear.

We now discuss the AB oscillations; the AR conductance as a function of magnetic flux ϕ is shown in figure 7. For simplicity, we set $n = \phi_R/\phi_L = 1$, $\varepsilon_1 = \varepsilon_2 = 0.1$, $t_c = 0.1$, and $\theta = \pi(\phi_R - \phi_L)/\phi_0 = 0$, respectively. The oscillation period of the AR conductance versus magnetic flux is 4π, which agrees well with the period formula $2\pi(n+1)$ for the N/DQD/S system [30]. When $R = 0$, the AR conductance presents a perfect AR process with the maximum value $4e^2/h$. When spin-flip scattering R increases, the amplitudes of the AR conductance decrease; at the same time, AR conductance shows more resonance peaks, which indicate more complicated electron tunneling. The spin-flip scattering cannot change the period of the AB oscillations but the phase of the AR conductance is reversed at $\phi = -2\pi, 0, 2\pi$ as soon as R exceeds some critical value. The AB oscillations are suppressed obviously by the spin-flip scattering.

The total flux ϕ or the flux difference θ between the left and right subrings can be used as a new type of swap operation in the DQD system. Two quantum states can be flipped by tuning the magnetic flux. To clearly show this swapping effect, we set the two quantum levels $\varepsilon_1 = 0.1$, $\varepsilon_2 = -0.3$, and $\theta = \pi/8$ ($n = 3/5$); figure 8 shows the AR conductance versus the gate voltage V_g. Due to the interdot coupling, the two quantum dot levels are renormalized, and the AR conductance shows a strong and a weak peak. When the total magnetic flux ϕ is varied from π to $-\pi$, the two peaks are

exchanged symmetrically, which indicates that the magnetic flux swaps the two states of the DQD. This means the bonding-like and antibonding-like states of the artificial molecule can be exchanged by adjusting the magnetic flux. This swap effect of the AR conductance may be used as a quantum bit in quantum computation [31, 32].

4. Conclusion

In conclusion, we have studied Andreev reflection and AB oscillations through a parallel-coupled double quantum dot system in terms of the nonequilibrium Green's function method. The AR conductance can be controlled in several ways, including the interdot coupling, the two quantum dot levels, the total flux, the flux difference between two subrings, the spin-flip scattering R and the gate voltage, respectively. Fano resonant peaks split and AB oscillation is suppressed due to the effect of the spin-flip scattering. It is also found that the bonding-like and the antibonding-like states, which result from the strong interdot coupling, can be swapped by changing the magnetic flux.

Acknowledgments

This work was supported by the National Natural Science Foundation of China (grant No 10674040) and Hebei Province Natural Science Foundation (grant No A2007000227).

References

[1] Aharonov Y and Bohm D 1959 *Phys. Rev.* **115** 485
[2] Sun Q F, Wang J and Guo H 2005 *Phys. Rev.* B **71** 165310
Sun Q F and Xie X C 2006 *Phys. Rev.* B **73** 235301
[3] Ji Y, Heiblum M, Sprinzak D, Mahalu D and Shtrikman H 2000 *Science* **290** 779
[4] Ji Y, Heiblum M and Shtrikman H 2002 *Phys. Rev. Lett.* **88** 076601
[5] Gerland U, Delft J V, Costi T A and Oreg Y 2000 *Phys. Rev. Lett.* **84** 3710
[6] Hofstetter W, König J and Schoeller H 2001 *Phys. Rev. Lett.* **87** 156803
[7] Lü H F and Guo Y 2007 *Phys. Rev.* B **76** 045120
[8] Entin-Wohlman O, Aharony A, Imry Y and Levinson Y 2002 *J. Low. Temp. Phys.* **126** 1251
[9] Kubala B and Koning J 2002 *Phys. Rev.* B **65** 245301
[10] Chung C H and Hofstetter W 2007 *Phys. Rev.* B **76** 045329
[11] Holleitner A W, Decker C R, Qin H, Eberl K and Blick R H 2001 *Phys. Rev. Lett.* **87** 256802
[12] Jiang Z T, You J Q, Bain S B and Zheng H Z 2002 *Phys. Rev.* B **66** 205306
[13] Lu H Z, Lü R and Zhu B F 2005 *Phys. Rev.* B **71** 235320
[14] Dong B, Djuric I, Cui H L and Lei X L 2004 *J. Phys.: Condens. Matter* **16** 4303
[15] Zhang G M, Lü R, Liu Z R and Yu L 2005 *Phys. Rev.* B **72** 073308
[16] Pan H and Lin T H 2006 *Phys. Rev.* B **74** 235312
[17] Zhu Y, Sun Q F and Lin T H 2001 *Phys. Rev.* B **65** 024516
[18] Cao X, Shi Y, Song X, Zhou S and Chen H 2004 *Phys. Rev.* B **70** 235341
[19] Peng J, Wang B G and Xing D Y 2005 *Phys. Rev.* B **71** 214523
[20] Li Y X, Choi H Y, Lee H W and Liu J J 2007 *J. Appl. Phys.* **101** 103918
[21] Blonder G E, Tinkham M and Klapwijk T M 1982 *Phys. Rev.* B **25** 4515
[22] Beenakker C W J 1997 *Rev. Mod. Phys.* **69** 731
[23] Khaetskii A V and Nazarov Y V 2000 *Phys. Rev.* B **61** 12639
[24] Petta J R, Johnson A C, Taylor J M, Laird E A, Yacoby A, Lukin M D, Marcus C M, Hanson M P and Gossard A C 2005 *Science* **309** 2180
DiVincenzo D P 2005 *Science* **309** 2173
[25] Cuevas J C, Martín-Rodero A and Yeyati A L 1996 *Phys. Rev.* B **54** 7366
[26] Yeyati A L, Cuevas J C, López Dávalos A and Martín-Rodero A 1999 *Phys. Rev.* B **55** R6137
[27] Pan H, Lin T H and Yu D 2004 *Phys. Rev.* B **70** 245412
[28] Sun Q F, Wang J and Lin T H 2000 *Phys. Rev.* B **62** 648
Sun Q F, Gao H and Wang J 2002 *Phys. Rev.* B **65** 075315
[29] Trocha P and Barnaś J 2007 *Phys. Rev.* B **76** 165432
[30] Zhang Y-P, Yu H, Gao Y-F and Liang J-Q 2005 *Phys. Rev.* B **72** 205310
[31] Loss D and DiVincenzo D P 1998 *Phys. Rev.* A **57** 120
[32] Hu X D and Das Sarma S 2000 *Phys. Rev.* A **61** 062301